Effect of arginine-rich cell penetrating peptides on membrane pore formation and life-times: a molecular simulation study

Sun, Delin; Forsman, Jan; Lund, Mikael; Woodward, Clifford E.

Published in:
Physical Chemistry Chemical Physics

DOI:
10.1039/c4cp02211d

2014

Effect of arginine-rich cell penetrating peptides on membrane pore formation and life-times: a molecular simulation study

Delin Sun,[a] Jan Forsman,[b] Mikael Lund, [b] and Clifford E. Woodward*[a]

[a]School of Physical, Environmental and Mathematical Sciences, University of New South Wales, Canberra ACT 2600, Australia

[b]Theoretical Chemistry, Chemical Centre, Lund University, P.O. Box 124, S-221 00 Lund, Sweden

* Correspondence: c.woodward@adfa.edu.au.

Abstract

The molecular basis for the effectiveness of arginine-rich cell penetrating peptides (ARCPPs) traversing cell membrane barrier is not well established. The fact that a threshold concentration of ARCPPs is required for efficient translocation in model membranes suggests cooperative action by ARCPPs. We used umbrella sampling simulations to calculate the free energies for membrane pore formation. The membrane-bound octaarginine (ARG8) peptides showed little cooperativity in lowering the free energy barrier to generate membrane pores by direct peptide translocation or by lipid flip-flop. Instead, high concentrations of ARG8 peptides were found to expand the surface area of the lipid bilayer due to the deep partitioning of guanidinium ions into the lipid glycerol regions. Surface-bound ARG8 peptides can also insert the arginine side chain into one existing transient membrane pore, and the lifetime of the transient membrane pore is significantly extended by arginine. This suggests a cooperative kinetic mechanism may act above a threshold adsorption concentration to facilitate the rapid uptake of these peptides.

1. Introduction

Eukaryotic cell membranes are natural barriers which inhibit the cellular uptake of certain small molecular drugs and large therapeutic agents, such as DNA and SiRNA.[1] To deliver these types of agents into the cytoplasm, safe and effective molecular carriers are needed. For some years now, it has been believed that this could be achieved via so-called cell penetrating peptides.[2] One example is the short arginine-rich transduction domain of the HIV-1 transactivator of transcription (Tat) protein.[3] The peptide sequence YGRKKRRQRRR (R=arginine, K=lysine, G=glycine, Y=tyrosine) was identified as key to the facilitation of cellular uptake of the Tat protein.[4] This discovery has sparked intense research interest in utilizing arginine-rich cell penetrating peptides (ARCPPs) as gene delivery carriers. Despite the enormous amount of work done to date, the molecular mechanism by which ARCPPs traverse the membrane barrier has not been established.

Early biological experiments found ARCPPs could be internalized in most eukaryotic cells even at low temperatures, i.e., in the absence of cellular energy.[4, 5] This finding suggested that cellular entry of ARCPPs did not involve endocytotic mechanisms. On the other hand, direct translocation through a lipid bilayer has an extremely unfavorable associated Born energy required and several non-endocytotic translocation models have been proposed to reconcile the experiments and theoretical predictions.[6, 7] However, the non-endocytotic translocation has been challenged by Richard and coworkers,[8] who showed that peptide uptake was significantly inhibited by low temperature or energy depletion. Thereafter, accumulating experimental evidence has begun to highlight the role of endocytotic pathways including macropinocytosis, clathrin-mediated endocytosis, and caveolae/lipid-raft-mediated endocytosis in facilitating cellular uptake of ARCPPs.[9-11] This notwithstanding, non-endocytotic pathways cannot be completely precluded. For example, experiments on giant unilamellar vesicles (GUVs) unambiguously showed that Tat peptides could pass through GUV bilayers without the aid of endocytosis.[12, 13]

A common feature shared by both endocytotic and non-endocytotic mechanisms is the requirement of negative Gaussian curvature of the lipid membrane, as has been shown by the seminal work of Wong *et al*.[13] Negative Gaussian curvature indicates saddle-splay structures, necessary for both water pore formation and membrane blebbing. The ability of ARCPPs to generate negative Gaussian curvature (and pores) has been ascribed to strong interactions between arginine and the phosphate group in lipids,[14] i.e, a guanidinium ion on arginine can form bidentate hydrogen bonds with a phosphate group. Solid-state NMR[15] and water/octanol partitioning experiments[16] support the potential role of bidentate hydrogen bonds. Another feature of ARCPPs is the apparent requirement of a threshold adsorption concentration on membrane surfaces,[9] which implies cooperative behavior of ARCPPs. This cooperativity has been explored with molecular dynamics (MD) simulations. Herce and García found that high concentrations of Tat and nona-arginine (ARG9) peptides could thin a dioleoylphosphatidylcholine (DOPC) lipid bilayer and generate water pores within a timescale of

200 ns.[7, 17] However, subsequent MD simulations by Yesylevskyy et al[18] have shown this is likely an artifact of improper electrostatic neutralization. Instead, it was postulated that Tat peptides are able to aggregate on dipalmitoylphosphatidylcholine (DPPC) membrane surfaces to alter the local membrane curvature. Experimental work by Ciobanasu *et al*[19] showed that surface diffusion rates of Tat peptides may indicate slow and fast modes, consistent with this hypothesis.

Many simulation studies on ARCPPs have focused on their ability to directly penetrate the membrane.[7, 20] The accompanying kinetic model generally assumes that peptide translocation is a quasi-equilibrium process (QEP), whereby the assumed faster modes of lipids, solvent and small solutes are averaged over. The QEP model implicitly assumes peptides penetrate the membrane via a sequence of independent events, with their efficacy stemming from a lowering of the translocation free energy via a (possibly cooperative) mechanism due to the adsorption of a sufficient number of peptides on the membrane surface. It is relevant to note then that recent simulation work by Huang and García has investigated the affect of adsorbed peptide on the free energy barrier for direct peptide translocation, which they found to be negligible.[20] As an aside, those authors also observed that a translocating peptide could sometimes cause a pore to form as it approached the bilayer center.[20] Not surprisingly, the free energy for this path was significantly lowered compared to a pore free one, but still remained high at around 100 kJ/mol. High activation free energies are typical in these types of calculations, implying peptide penetration (even via pore forming paths) remains a relatively rare event. This is not surprising as ARCPPs generally carry significant positive charges, and the translocation free energy is dominated by the desolvation of the peptide.

It is possible that pore forming events in a lipid bilayer can occur spontaneously. Simulations by Bennett et al have shown that pores may be induced in zwitterionic lipid bilayers via a lipid flip-flop mechanism.[21] The free energy for this process is also found to be very high (around 80 kJ/mol for DPPC), which implies that the pore density on the bilayer surface should be low. It is interesting to consider the influence of adsorbed peptide on the stability of such pores. If pores are made more stable, they will have a higher concentration in the bilayer and allow a higher rate of peptide translocation. However, in the context of the QEP model, any thermodynamic advantage realized via this scenario should be revealed in the free energy of direct translocation in the presence of adsorbed peptide, provided translocation proceeds via a proper equilibrium path and is not subject to non-ergodic effects. As described by Huang and García, the sampling of phase space in simulations of finite length may well be incomplete. [20] Furthermore, while thermodynamic factors, which stabilize pores, pertain to the ratio of pore opening and closing rates, additional kinetic effects may affect the rate of the closing of a pore, once it is open. When strong peptide lipid interactions are present it is possible that the peptide will affect the local lipid dynamics, that is, the kinetics of lipids will be influenced by the timescale of peptide relaxation events. This is especially so for bilayer regions of negative Gaussian curvature (such as pores), which experiments suggest are points of large accumulation for ARCPPs. If this is the case, the QEP model may no longer be justified. Peptide translocation is inherently a dynamic phenomenon and if the lifetime of pores is linked to the timescale of peptide dynamics, different

translocation kinetics may be manifested. Indeed, an analysis presented later will reveal that prolonged pore lifetimes, caused by either thermodynamic or kinetic factors (or both), can result in very efficient peptide translocation, when the peptide adsorbed on the outer leaflet is above a critical peptide to lipid ratio.

The aim of the work presented here is to use molecular dynamics (MD) simulations to investigate the influence of ARCPPs on the stability and kinetics of pores in a lipid bilayer. While the influence of adsorbed peptide on the formation of pores in the first place is of course relevant and important, a major part of our investigation will focus on the effect of adsorbed peptides on pores, *once they have formed*. MD may uncover both thermodynamic and kinetic factors, both of which may play a role when peptide associates with lipid molecules. The experimental evidence suggests that significant peptide adsorption is a necessary requirement for efficient translocation and arginine is a likely candidate, given its potential to form bi-dentate H-bonds with lipid head groups. A model that displays these strong interactions will be described below. We study the effect of adsorbed peptide on the equilibrium bilayer, which allows us to compare our model with other similar simulation work and available experimental data. Following the work of Huang and García[20], we used umbrella sampling simulations to also investigate the role played by adsorbed peptide on direct peptide translocation. Similar methods were also used to study the effect of peptide adsorption on the free energy of pore formation by lipid flip-flop. Finally, the life-time of pores, once they had formed, was measured. The implications of increasing pore life-times on peptide movement through membranes are discussed, wherein, we propose that cooperative peptide diffusion through nucleated pores is a possible explanation for the rapid translocation of ARCPPs.

2. Methods

2.1 Peptides and lipid bilayer models

It has been known that oligoarginines with 7-15 residues exhibit a superior cellular uptake rate than the Tat peptide.[16, 22] In this work, an atomistic model of ARG8 peptide was used in MD simulations in order to study the interaction mode of arginine-rich peptide to a DPPC lipid bilayer. In the ARG8 peptide model, all guanidinium groups were protonated whereas the termini of peptides were considered as neutral. The fact that a single mutation of aginine in the Tat peptide could dramatically affect the peptide's membrane permeation ability[14] implies that terminal charges of arginine-rich peptides are not the determinant factor. A given peptide was firstly simulated in a cubic periodic box in the presence of 4,000 water molecules and eight chloride counter-ions for 10 ns in an NPT ensemble. In this way, an equilibrated structure of ARG8 was obtained for the subsequent bilayer-peptide simulations. The initial configuration of the DPPC bilayer (128 lipids) was downloaded from http://www.softsimu.net/downloads.shtml. The DPPC bilayer was solvated by 6400 water molecules in a 6.4 nm× 6.4 nm × 8.4 nm rectangular simulation box with periodic boundary condition in three dimensions. In this work, unless otherwise specifically stated, all lipid bilayers contain 128 DPPC lipids.

2.2 Steered MD and umbrella sampling simulations

Steered MD[23] and umbrella sampling simulations[24] were performed to study the effect of membrane-bound ARG8 peptides on the free energies for generating membrane pores by direct peptide translocation and by lipid flip-flop. In steered MD simulations, a harmonic potential with a force constant of 1000 kJ/mol/nm^2 was applied between the center of mass of one peptide (or lipid head) and one reference point determined with respect to the center of mass of the lipid bilayer. The peptide (or lipid head) was pulled along the z-axis (perpendicular to the membrane) from the bulk water (or bilayer/water interface) to the bilayer center at a rate of 0.01 nm/ps. Configurations from steered MD simulations were selected every 0.1 nm along the z-axis and used as starting points for umbrella sampling simulations. 32 windows were generated for peptide translocation simulations and 25 windows were generated for lipid flip-flop simulations. Starting from the configuration in which one lipid head was constrained in the bilayer center, umbrella sampling simulations were also performed by pulling the lipid head back from the bilayer center to the bilayer/water interface. The total umbrella simulation time was 12.65 μs (see Table 1 for details). In the umbrella sampling simulations, a biased harmonic potential with a force constant of 3000 kJ/mol/nm^2 was used to confine the peptide or the lipid head within the sampling window. In this way, the unbiased probability distribution functions can be obtained for each window to construct the PMF profile using the weighted histogram analysis method (WHAM).[25]

2.3 Unconstrained MD simulations

Unconstrained MD simulations were performed to investigate the interaction mode of a finite concentration of ARG8 peptides to the DPPC lipid bilayer. Nine simulation systems were constructed for the simulations, as is listed in Table 1. For the cases A1O-A4O, the peptides were all initially inserted close to one leaflet of the bilayer to allow them to preferentially adsorb to that leaflet, which they did spontaneously. For systems A2T-A8T, peptides were evenly distributed on both sides of the bilayer. Water molecules which were initially within 0.15 nm of the inserted peptides were deleted and chloride ions were added to neutralize the systems. Most simulations were run for 200 ns. The larger system (512 lipids and 16 ARG8 peptides) was run for only 50 ns.

Unconstrained MD simulations were also performed in order to study membrane pore closure (see Table 1). In the case of membrane pore formed by peptide translocation during umbrella sampling simulations, at the end of the umbrella sampling process, the ARG8 peptide at the center of the pore was removed and 200 ns of unconstrained MD simulations were run for the rest of the system. Similarly, for membrane pores induced by lipid flip-flop in umbrella sampling simulations, the bias force exerted on the lipid head was removed and 200 ns unconstrained MD

simulations were run. In this way, the effect of membrane-bound ARG8 peptides on the membrane pore closure rate was investigated.

2.4 Force field and simulation parameters

In this study we shall adopt a force-field model that has been extensively used for the study of cell penetrating peptides interacting with zwitterionic lipid bilayers.[7, 18, 26, 27] This model combined the Berger lipid model[28] with the GROMOS peptide model, which gives rise to relatively strong adsorption for the latter in the absence of additional electrolyte. Recent work by Vazdar et al[29] and MacCallum et al [30] have instead used an OPLS-AA force field for arginine combined with a Berger model for zwitterionic bilayers. MacCallum et al, using the OPLS-AA/Berger combination, to predicted that a single arginine side chain interacts very strongly (-21.2 kJ/mol) with a zwitterionic DOPC lipid bilayer in the absence of salt[30]. This is somewhat stronger than that predicted by the force-field combination used in our study. On the other hand, Vazdar et al[29] predicted weak interactions for deca-arginine with a zwitterionic POPC lipid bilayer with an OPLS-AA/Berger force field combination, but in the presence of 0.125 M NaCl. It seems likely that the added salt gives very pronounced screening of the electrostatic peptide lipid interactions. With this in mind, in this work, the force field used to describe the DPPC lipid bilayer was taken from Berger *et al*.[28] The ARG8 peptide was described with the GROMOS53a6 force field.[31] The simple point charge (SPC) model[32] was used to model water. Furthermore, only counterions were present to maintain electroneutrality and there was *no added salt*.

All simulations were performed at a temperature of 323K which is above the main phase transition temperature of the DPPC bilayer (314K).[33] All molecular species were independently coupled to the Nosé-Hoover thermostat[34, 35] with a coupling time constant of 0.5 ps. The system's volume was allowed to fluctuate according to the semi-isotropic pressure coupling method. Here, the lateral and perpendicular pressures (both 1atm) were independently coupled to the Parrinello-Rahman barostat[36] with a coupling time constant of 2 ps and compressibility of 4.5×10^{-5} bar^{-1}. Periodic boundary conditions were employed. A cutoff of 1 nm was employed for the non-bonded Lennard-Jones and the real-space part of electrostatic interactions. Long-range electrostatic interactions were treated using the particle-mesh Ewald (PME) method[37] with a Fourier spacing of 0.15 nm. The neighbor lists were updated every 10 steps. We found this treatment of non-bonded interactions could accurately predict the experimental area per lipid of the DPPC bilayer. All bonds lengths in peptides and lipids were constrained using the LINCS algorithm[38] and SPC water molecules were constrained using the SETTLE algorithm.[39] The simulation time step was 2 fs. Simulations were performed using the GROMACS 4.5.4 package.[40]

3. Results

3.1 Membrane pore generation by peptide translocation and lipid flip-flop

Experimental studies suggest that ARCPPs can generate membrane pores in synthetic lipid vesicles.[12, 13, 41, 42] In molecular simulation studies, membrane pores can be generated in many different ways including: cationic peptide translocation;[18, 20] lipid flip-flop;[21] mechanical stress;[43] direct application of an electric field,[43] and ionic charge imbalance.[44] Here, we used two methods, direct peptide translocation and lipid flip-flop to generate membrane pores. In the first case, the distance between the center of mass of the peptide and the bilayer center was chosen as a reaction coordinate for umbrella sampling simulations. In the second case, the distance between the head group of a tethered lipid and the bilayer center was used. A potential of mean force (PMF) profile was calculated using umbrella sampling.[18, 20, 21] Our goal was to determine whether adsorbed ARG8 peptides on the outer leaflet, would significantly affect the resulting PMF.

Table 1 Simulation systems

Umbrella sampling simulations					Unconstrained simulations			
System	No. of peptide[a]	No. of lipid	No. of umbrella windows	Simulation time per window (ns)	System[b]	No. of peptide[a]	No. of lipid	Simulation time (ns)
Peptide translocation-1	0	128	32	100	A1O	1	128	200
Peptide translocation-2	4	128	32	100	A2O	2	128	200
Lipid flip-flop-1	0	128	25	50	A3O	3	128	200
Lipid flip-flop-2	4	128	25	100	A4O	4	128	200
Reverse lipid flip-flop-1	0	128	25	50	A16O	16	512	50

Reverse lipid flip-flop-2	4	128	25	50	A2T	2	128	200
					A4T	4	128	200
					A6T	6	128	200
					A8T	8	128	200
					Peptide translocation-1	0	128	200
					Peptide translocation-2	4	128	200
					Lipid flip-flop-1	0	128	200
					Lipid flip-flop-2	4	128	200

[a]No. of peptide means the number of peptide on bilayer surface. [b]A is abbreviated for arginine, O means all peptides were placed on one leaflet of bilayer and T means all peptides were evenly placed on two leaflets.

The PMF profiles for ARG8 translocation through DPPC lipid bilayer are plotted in Fig. 1. Pore formation is directly observed (via snapshots of the system) at separations corresponding to the "kink" in the PMF, when the peptide is close to the bilayer center. This kink indicates a crossing from a pore-free to a pore-formed branch of the free energy profile. The activation free energy for membrane pore generation is defined as the difference between the free energy at this crossing point (approx. 0.6 nm), and the minimum in the PMF. When the PMF is generated in the absence of adsorbed peptide, the activation free energy is 87.5 kJ/mol. If four additional ARG8 peptides are adsorbed onto the outer surface, we note the following changes to the PMF. Firstly, the free energy minimum at the lipid/water interface is significantly smaller (approximately -20kJ/mol). Thus, peptide lipid interactions are significantly weakened by the presence of other adsorbed peptide. This is likely due to the mutual electrostatic repulsion between peptides at the surface. Secondly, the PMF remains higher than in the case where additional peptide is not adsorbed and the activation free energy for pore generation increased slightly to 89.0 kJ/mol. These results are very similar to those reported by Huang and García, who studied cyclic ARG9 peptide with the DOPC lipid bilayer.[20]

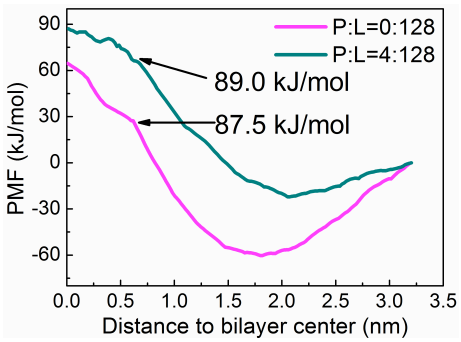

Fig. 1 Free energy profiles for transferring one ARG8 peptide from water to DPPC lipid bilayer center.

Our calculations imply that adsorbed ARG8 peptides do not cooperate to significantly lower the barrier for pore formation by direct peptide translocation. However, meta-stable pore-free and pore-formed states are suggested by the kink in the PMF. As pointed out by Huang and García,[20] pulling a peptide through the bilayer past the true branch crossing point (along a meta-stable pore-free path) may lead to an overestimation of the free energy of pore formation. For this reason, we decided to consider another pore generating method, that constraints lipid movement to some extent.

As has been shown in recent umbrella sampling simulations,[21] the translocation of a single lipid molecule through a bilayer (as would occur during a flip-flop process) is sufficient to induce pore formation when the lipid approaches the bilayer center. Fig. 2 (a) shows the PMF profiles that arise from the pulling of a single DPPC lipid head through the bilayer. We ran two sets of umbrella sampling calculations. In one case, we used 50 ns per sampling window, and in the other we used 100 ns. Both gave quantitatively similar results, and we have only shown the calculations due to the longer simulations. As with the case of peptide translocation, these simulations were performed both with and without additional ARG8 adsorption to the outer leaflet. Without adsorbed peptide, the activation free energy for membrane pore generation is 76 kJ/mol, with the pore forming when the head of the tethered lipid is approximately 0.25 nm from the bilayer center. With peptide adsorbed (P/L = 4/128), the free energy barrier decreases, but only by approximately 1.0 kJ/mol. These results suggest that adsorbed peptide only marginally affects the free energy of pore formation by lipid flip-flop. However, the possibility remains that these free energy estimates could be artificially high, due to the presence of hysteresis. Hence, we performed umbrella sampling simulations whereby the tethered lipid molecule was pulled back along a reverse path. We found that when peptide is absent, the forward and reverse paths seem reversible (Fig. 2 (b)), with pore closure occurring at about the same distance as in the forward path. On the other hand, in the presence of the adsorbed peptide, the pore persisted initially for a significantly longer distance (approx. 0.7 nm) from the bilayer center, compared to the forward path. We also observed, pore re-opening at larger separation (1.5 nm). This result indicates that, once a pore is formed by lipid flip-flop with adsorbed peptide, the presence of the tethered lipid (which initiated pore formation) was no longer required to keep the pore open.

Instead, the adsorbed peptide is able to maintain the pore. The large hysteresis indicates kinetic barriers to pore closure are enhanced by adsorbed peptide and that the actual crossing point of the free energy branches may occur somewhere between 0.25 – 0.7 nm. From Fig. 2 (a), this corresponds to a free energy difference of up to 50 kJ/mol.

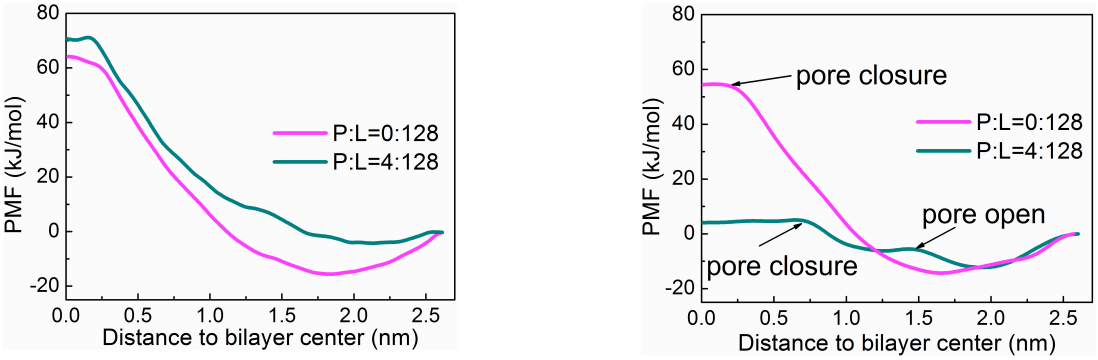

(a) (b)

Fig. 2 (a) Free energy profiles for transferring one DPPC lipid head from bilayer/water interface bilayer center. (b) Free energy profiles for transferring one DPPC lipid head from bilayer center to bilayer/water interface.

3.2 Unconstrained molecular simulations of membrane adsorbed ARG8 peptides

While this study is primarily concerned with the translocation process, it is also relevant to investigate the way adsorbed ARG8 peptide affects the equilibrium structure of an intact lipid bilayer. Comparisons with other similar modeling studies and available experimental data is also useful in the evaluation of our model.

To obtain the results reported in this section, asymmetric bilayers were created by inducing a number of peptides to adsorb onto the "outer" leaflet only at various peptide to lipid ratios (see Table 1). After 200 ns of unconstrained MD simulations, we did not observe the formation of either membrane pores or any other type of obvious membrane defects in any of our systems. Instead, we found that ARG8 peptides preferred to adsorb onto the bilayer/water interface. Our results are consistent with simulation studies of Yesylevskyy *et al*[18] which did not detect any membrane defect in DOPC and DPPC bilayers in the presence of Tat peptides. However, as is discussed later, adsorption increases the surface tension of the inner leaflet, promoting the possibility of pore formation. In simulation work of similar nature, Li *et al*[45] observed the appearance of membrane pores over a short time. However, their result is likely due to a charge imbalance, which occurs across the asymmetric bilayers, created by the use of only (positive) counterions to the negatively charged inner leaflet.

In the work of Yesylevskyy *et al*,[18] MD simulations on a large system containing 512 DPPC lipids and 8 Tat peptides were also performed. After 50 ns, the Tat peptides were found to aggregate on the bilayer surface and induced a membrane undulation, which suggested the onset

of micropinocytosis.[18] To test whether such a mechanism was present in our system, we scaled up system A4 (Table 1) to generate a larger simulation box containing 512 DPPC lipids and 16 ARG8 peptides and performed MD simulations for 50 ns. In contrast to the case of Tat peptides, we found that the ARG8 peptides remained separated on a virtually planar lipid bilayer.

Despite the fact that membrane pores were not observed in our simulations, mounting experimental evidence supports the occurrence of membrane pores as the major non-endocytotic entry route of ARCPPs. In particular, experimentalists have detected water columns across model membranes incubated in Tat peptide solutions.[46] Of course, the likely reason that we did not find membrane pores is that the maximum time for the MD simulations we performed was only 200 ns. Experimentally, the timescale required for internalization of ARCPPs is on the order of minutes.[2] We also note that in our simulations, a pure DPPC bilayer was used. Independent experiments by Ciobanasu *et al*[12] and Mishra *et al*[13] showed that Tat peptides did not appear to generate membrane pores in GUVs composed purely of PC lipids. Instead, anionic phosphatidylserine (PS) lipids or neutral phosphatidylethanolamine (PE) lipids (with negative intrinsic curvature) appeared necessary for membrane water pore formation. In this regard, the molecular action of Tat peptide is analogous to antimicrobial peptides, which are known to disrupt PE-rich cell membranes.[47] Thus, bilayer composition likely plays some role in determining the propensity to form membrane pores.

3.3 Hydrogen bonding analysis

The superior cellular uptake rate of ARCPPs has sometimes been ascribed to the ability of the guanidinium ion forming bidentate hydrogen bonds with phosphate groups on the lipid head.[14] Quantum mechanical calculations have confirmed that these bidentate hydrogen bonds do form.[48] We analyzed the hydrogen bonding between guanidinium ions and lipids in our simulations, using the following geometric criteria:

(i) the donor-acceptor atom distance is not longer than 0.35 nm.

(ii) the donor-hydrogen-acceptor atom angle is not greater than 30°.

Our simulations indicate that the guanidinium ion can indeed form bidentate hydrogen bonds with the phosphate of the lipid head. In addition, guanidinium ions are also able to form hydrogen bonds with the lipid glycerol groups. We plotted the total number of hydrogen bonds formed between the 32 guanidinium ions (on the 4 peptides) and the 64 lipids, see Fig. 3. Guanidinium ions form approximately equal numbers of hydrogen bonds with the phosphate and glycerol groups. This concurs with solid-state NMR experiments, which showed arginine rich Tat peptides are deeply embedded in the lipid glycerol regions.[49]

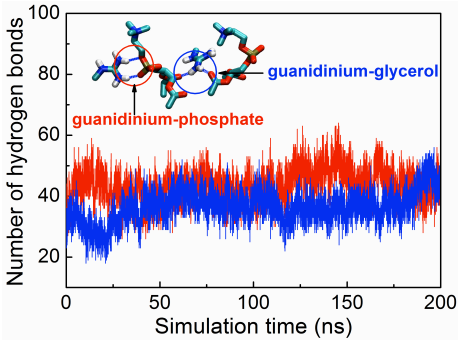

Fig. 3 Time evolution of the number of hydrogen bonds formed between guanidinium ions on 4 peptides and phosphate, glycerol groups on 64 lipids.

3.4 Effect of ARG8 peptides on the structural properties of the bilayer

While previous simulations of membranes bound Tat peptides[7] may have exaggerated their effect, membrane expansion and consequent thinning have been suggested as a common mechanism by which membrane active peptides, including antimicrobial and amyloidal peptides, can disrupt the bilayer and form membrane pores.[50, 51] It has been reported that antimicrobial peptides can induce positive curvature strain on lipid bilayers[52, 53] whereas amyloid peptides mainly induce negative curvature strain.[54] On the other hand, the Tat peptide is capable of inducing both positive and negative curvature on a bilayer.[13, 14] It is plausible that all these membrane active peptides utilize common mechanisms to disrupt cell membranes.

We examined the effect of adsorbed ARG8 peptides on the structural properties of the DPPC bilayer including: area per lipid, bilayer thickness, and lipid alkyl chain order parameters. We considered either all peptides being placed on one leaflet (asymmetric) or peptides being evenly distributed between both leaflets (symmetric). The subsequent areas per lipid for varying numbers of ARG8 peptides are given in Figs. 4 (a, b). For both asymmetric and symmetric cases, the area per lipid increases in the presence high concentration of ARG8. The mechanism for this is likely the partitioning of the guanidinium ions deep into the lipid glycerol region. The bilayer also changes its thickness, as shown in Fig. 5, which plots the phosphorous electron density profiles to indicate bilayer thickness. The adsorption of four ARG8 peptides on each leaflet reduces the average bilayer thickness by 2Å. This is consistent with recent neutron diffraction experiments by Chen et al.[46] who found that Tat peptides caused thinning of bilayers.

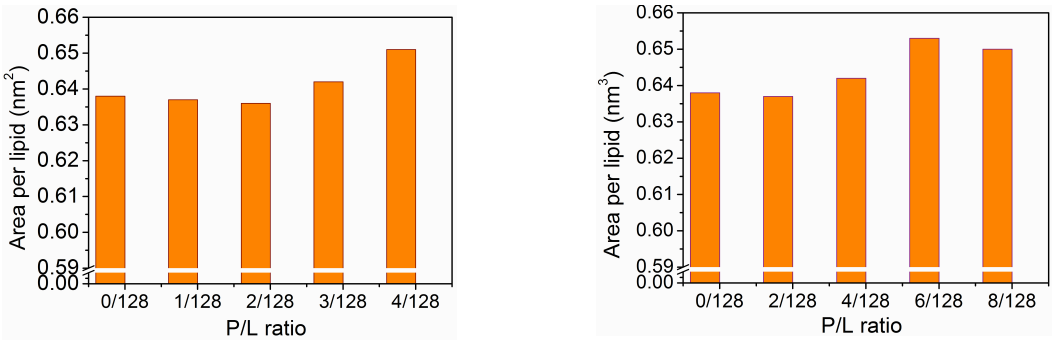

(a) (b)

Fig. 4 Area per lipid of DPPC bilayer in the presence of varying number of ARG8 peptides. (a) All peptides were adsorbed onto one leaflet of bilayer. (b) Peptides were evenly distributed on both leaflets. P/L ratio represents the number ratio of peptide and lipids in the simulation system. The area per lipid was obtained from the last 100 ns MD simulation data.

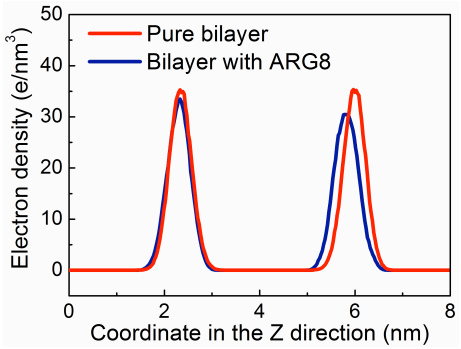

Fig. 5 Electron density profiles for phosphorus atoms on lipid heads. The profiles were obtained from the last 100 ns MD simulation data for system A8T.

The changes in bilayer area and thickness also correlate with changes to lipid ordering as well. The alkyl chain order parameter is defined as

$$S = \frac{1}{2}\left(3\left\langle \cos^2 \theta_n \right\rangle - 1\right) \qquad (1)$$

where θ_n is the angle between the bilayer normal and the nth segmental vector (linking the n-1 and n+1 carbon atoms in the lipid chain) and bra-ket notation is used for the ensemble average. A decrease in S_n means the lipid packing becomes orientationally more disordered. Fig. 6 shows the calculated order parameter profiles both without adsorbed peptide, and with peptide on both surfaces. Adsorbed ARG8 tends to disorder alkyl chain packing. It has been argued in recent studies[55] that this disordering effect may increase the fluidity of the lipid bilayer and facilitate the formation of membrane pores.

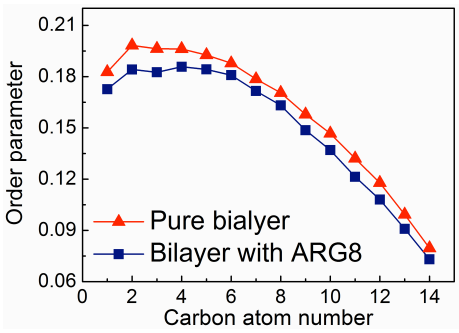

Fig. 6 Calculated order parameters versus different carbon atoms on lipid alkyl chain. The profiles were obtained from the last 100 ns MD simulation data for system A8T.

3.5 Effect of ARG8 peptides on membrane pore kinetics

Our results show that the activation free energy for generating membrane pores by single peptide translocation and by lipid flip-flop were not very different (87.5 kJ/mol *vs* 76.1 kJ/mol). The similarity of these values is consistent with the non-additive transfer model proposed by MacCallum *et al*.[56]

In the case of no adsorbed peptide, we found that a pore generated by lipid flip-flop was very short-lived. This was determined by performing unconstrained simulations at the conclusion of our umbrella sampling calculations. That is, unconstrained simulations were carried out upon releasing the tethered lipid after its translocation to the bilayer center. Pore closure occurred after only 5 ns of simulation time (see Fig. 7 (a)), which is consistent with recently reported simulations[21] using similar models and methods. Hence, pores formed by random lipid fluctuations in an isolated DPPC bilayer have a relatively short lifetime. This result is also consistent with the results of our reverse pulling umbrella sampling simulations presented above (Fig. 2 (b)). On the other hand, pores formed by translocation of an ARG8 peptide to the bilayer center persisted for the full length of similar unconstrained simulations (200 ns). This was the case, even though the pore forming peptide was deleted before the unconstrained simulations were carried out (Fig. 7 (b)). Clearly, the ARG8 peptide is able to create a much more stable pore, relative to that formed by lipid flip-flop. Not surprisingly, when adsorbed peptide is present on the outer leaflet, pores formed by peptide translocation also persisted for the full length of the subsequent 200 ns of unconstrained simulation (Fig. 7 (c)). During the unconstrained simulations, we noted that an adsorbed peptide molecule partially entered the persistent pore via surface diffusion. This behavior is consistent with a relieving of the increased positive tension on the outer leaflet. This suggests an effective "attraction" between adsorbed ARG8 peptides and transient pores. Similar behavior may also be expected in the presence of other surface heterogeneities, which effectively increase the surface area of the outer leaflet.

Finally, we carried out unconstrained simulations on pores generated by lipid flip-flop in the presence of adsorbed peptide. We found that the life-time of these pores was also extended to at least the full simulation length of 200 ns, with no sign of pore closure. During the unrestrained

simulations we again noted that one of the adsorbed ARG8 molecules partially entered the pore (Fig. 7 (d)). The presence of this peptide was sufficient to maintain the pore over the duration of the simulation. Again, this result is consistent with the reverse pulling umbrella simulations presented earlier (Fig. 2 (b)). The presence of adsorbed peptide appears to stabilize the pores and prolong their life-time significantly.

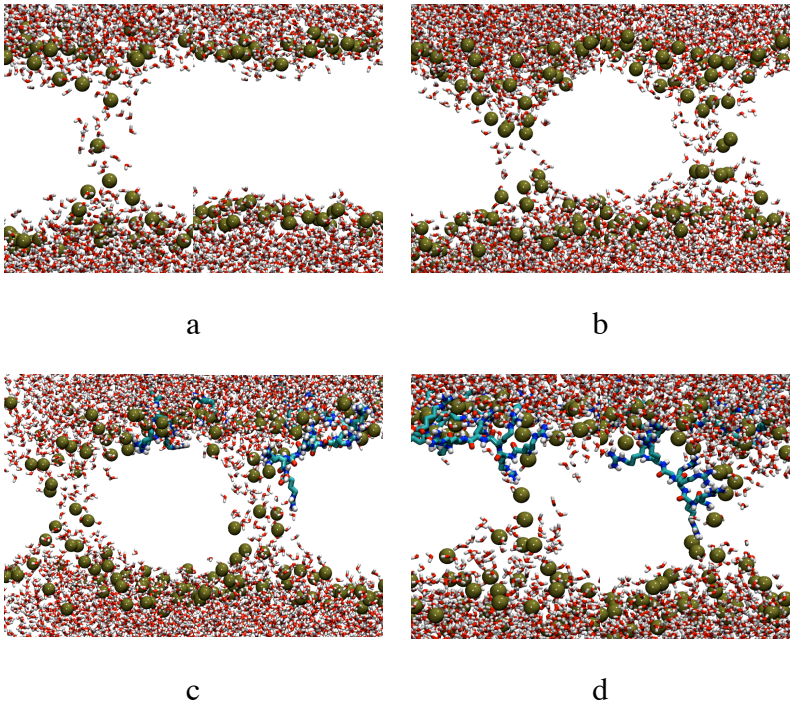

Fig. 7 The starting configuration of membrane pores and fates of membrane pores after 200 ns unconstrained MD simulations. (a) The membrane pore was generated by lipid flip-flop without peptide adsorbed on the membrane surface. The pore closed quickly after 5 ns. (b) The membrane pore was generated by peptide translocation without peptide adsorbed on the membrane surface. After 200 ns MD simulations, the pore remained open. (c) The membrane pore was generated by peptide translocation with four peptides adsorbed on the membrane surface. After 200 ns MD simulations, the pore remained open and one ARG8 peptide started to insert into the pore. (d) The membrane pore was generated by lipid flip-flop with four peptides adsorbed on the membrane surface. One arginine side chain inserted itself into the pore and kept the pore open after 200 ns of MD simulations.

4. Discussion

4.1 Adsorbed ARG8 peptides induce internal membrane tension

Though our major focus in this work concerns the life-time of membrane pores, our results on peptide adsorption on the intact bilayer prompt us to speculate on the factors which may facilitate initial pore formation.

The unconstrained MD simulations we performed suggest that the asymmetric adsorption of a high concentration of ARG8 peptides on the outer leaflet creates expansive forces there. These peptides are attracted to the bilayer surfaces as evidenced by our simulations, which show hydrogen bonding between the ARG side chains and both the phosphate and glycerol regions of the lipid molecules. The expansive forces on the outer leaflet, bring about a curvature strain on the bilayer. However, confined by the simulation box, the bilayer expands to form a "frustrated" structure. A similar scenario would also apply to the case of a vesicle. The result is an excess positive surface tension on the inner leaflet (and an opposing negative surface tension on the outer one). One way to relieve this frustration is for the flat bilayer to open a water pore. From Fig. 4 (a), we see that when the P/L ratio is 4/128, the fractional change of bilayer surface area f_S is approximately 0.02. The intrinsic surface tension, σ, induced on the inner leaflet can be estimated as

$$\sigma = \frac{1}{2} k_a f_S \qquad (2)$$

k_a =0.24 N/m is the stretch modulus of the DPPC lipid bilayer,[51] which gives $\sigma \approx 2.4$ mN/m. Even this small membrane tension is sufficient to mechanically destabilize the membrane and create membrane pores in fluid lipid vesicles. For example, Zhelev and Needham's experiments showed that the critical membrane tension to porate SOPC lipid vesicles was in the range of 1-2.8 mN/m.[57] However, it is worth noting that pore formation may not necessarily be the only way to relieve a frustrated bilayer structure. For a giant vesicle with diameter of 50 μm, the expansion of the outer leaflet in the ARG8 case considered above would be around 6×10^8 nm^2. This dramatic surface area change may be sufficient to induce vesicle budding or some other membrane remolding.[58, 59]

A similar mechanism for antimicrobial peptides has been proposed by Huang *et al*.[60] In this case, a "two-state" model has been suggested for the orientation of adsorbed peptide (S-state: peptides are parallel to the membrane surface and I-state: peptides are perpendicular to membrane surface). In this theory, a threshold peptide concentration is crucial to produce a sufficiently large membrane surface tension in order to facilitate the formation of membrane pores with a concomitant change in the average peptide orientation from S to I, as they act to stabilize the pores. According to the model, the internal membrane tension induced by antimicrobial peptides could reach as large as 5-15 mN/m.[61] These peptides may also promote pore expansion. For example, Rakowska et al. found that an induced membrane pore can promote antimicrobial peptides to constantly migrate from membrane surface to pore edges, leading to an expansion of the membrane pore to micrometer scales.[62]

While our unconstrained MD results displayed membrane expansion and thinning by adsorbed ARG8 peptides, no pores were actually observed during the 200 ns of simulation time. Indeed, our umbrella sampling simulations did not indicate substantial stabilization of pores by adsorbed

peptides. However, the free energy lowering imparted by adsorbed peptide remains uncertain, due to substantial hysteresis effects, which persisted even in our longer umbrella sampling simulations for lipid flip-flop. The PMF for inward translocation of the lipid molecule showed branch crossing from a pore-free to a pore-formed state when the lipid was close enough to the membrane center. Reverse pulling simulations indicated that the pore-formed state persisted at much greater distances from the membrane center of the constrained lipid, when compared with the inward journey. A proper evaluation of the relative free energies of pore-formed and pore-free states will require much longer simulation times than have been made available for the current work.

4.2 Adsorbed ARG8 peptides slow down pore closure

It is clear that the presence of bound peptides on the outer surface of the membrane significantly increases the life-time of transient pores, once they are formed. As shown in our unconstrained simulations, following the formation of a pore by lipid flip-flop, adsorbed peptide prolonged the life-time of pores to at least 200 ns (see Fig. 7 (d)) and likely much longer. This is to be compared with the typical 5 ns life-time of pores in the absence of peptide. It is not clear whether this is largely a thermodynamic effect (due to lowering of the free energy of the pore) or a kinetic effect, with the peptide dynamically slowing down the rate of closure. While much recent theoretical work concerning peptide effects on pores has focused on thermodynamic stabilization, it is likely that both kinetic and thermodynamic factors come into play.

During the unconstrained simulations, one of the adsorbed ARG8 molecules partially entered the pre-formed pore. It would appear that once at the mouth of the pore, this peptide essentially anchors some of the lipid molecules near the rim and this is sufficient to prolong the lifetime of the pore. Our results suggest that a major point of peptide adsorption appears to be deep in the glycerol region of the bilayer, imparting expansive forces to the membrane at the pore edge. We conjecture that a pore closes via cooperative motion of lipids and this process is likely initiated at the pore edge. The presence of a peptide, if strongly associated with the lipids would slow such a process down, so that it would occur on the time scale of peptide diffusion. That is, if the peptide were to diffuse away, the pore would presumably close relatively quickly. However, mass action and expansive forces, due to excess peptide adsorption on the outer surface, would instead cause the peptide to penetrate further into the pore, where it continues to prevent pore closure. It is relevant to note in this context, that just a single lipid molecule held by the peptide in the vicinity of the bilayer center would be sufficient to nucleate (or maintain) a membrane pore, as evidenced by our lipid flip-flop umbrella simulations. Hence, pore closure will eventually occur only once that peptide had translocated to the other side of the bilayer and diffused away from the pore edge on the inner leaflet. We did observe that over the 200 ns of simulation, the pore-associated peptide did diffuse further into the pore, but translocation was not completed over this time. While it would seem that strong peptide-lipid interactions are required to achieve this effect, we note that in the model used here, the free energy of bilayer association of peptide is low (approximately -3kJ/mol per arginine residue when P/L = 4/128). Hence, this effect is present

even when the effective peptide-lipid interactions are relatively weak. On the other hand, the cooperative effect of the oligoarginine chain clearly plays an important role. As is also confirmed in experiments, which show that oligoarginines with at least 7 residues are required to exhibit good cellular uptake.[16, 22]

Peptide translocation through a formed pore is the core idea behind the recent model of Huang and García,[20] who conjectured that lipid pore states contribute significantly to the translocation path of peptides. Here it is assumed that the pore kinetics is fast compared to that of peptide diffusion, so that an appropriate reaction coordinate is assumed pinned to the peptide, and pre-averaging of the partition function over the orthogonal (assumed fast) degrees of freedom provides a PMF (e.g., see Fig. 1) on which peptide diffusion kinetics takes place. This is the so-called QEP model described earlier. The rate of translocation was estimated by assuming that each peptide diffuses through these transient pores independently of other peptides and that after a peptide molecule translocates, the pore closes rapidly. Hence, the population of transient pores is essentially at equilibrium. In the context of this approach, thermodynamic stabilization of pores by adsorbed peptide can explain enhanced uptake of peptides due to the subsequent greater concentration of available pores. An increase in the equilibrium concentration of transient pores requires a mechanism for thermodynamic stabilization of pores by adsorbed peptide, which our umbrella sampling simulations suggest may not occur. Though, hysteresis effects suggest a more careful study should be performed. It is worth noting that the two-state model due to Huang (appropriate to antimicrobial peptides) postulates the existence of non-transient pores, stabilized by resident peptides, beyond a critical adsorption ratio of number of peptides to lipid.[61] In this regime, pores are stabilized to the extent that they will remain open, while the peptide concentrations on both sides of the bilayer reach their equilibrium values. The possibility of this occurring for transient pores is now explored.

4.3 A cooperative kinetic model for rapid peptide translocation

Our simulation results indicate that a peptide molecule at the entrance to a pore is sufficient to prolong its life-time, so that thermodynamic forces (mass action and expansion) will induce it to translocate. There exists a concentration regime of adsorbed peptide where this effect can lead to enhanced peptide translocation via a cooperative kinetic mechanism. This occurs when the time for a peptide to cross a pore, τ_{tr}, is similar to or greater than the time it takes for a peptide molecule on the surface to diffuse to an available pore, τ_d. A crude estimate for translocation time is $\tau_{tr} \sim H^2/D_p$, where H is the typical length of a pore (~4 nm) and D_p is the surface diffusion coefficient of the peptide. Despite the fact that the pore is already formed, a free energy barrier to translocation exists due to partial desolvation of the peptide within the pore. This effect would serve to increase the translocation time, but we ignore it here.

The time taken for peptide on a surface to diffuse to a pore can be estimated as follows. We assume simple two-dimensional Fickian diffusion on the membrane surface whereupon a steady state, radially symmetric, diffusion current of peptide has been established. The peptide

concentration has its average value c_p at some outer radius r_o and is zero at the pore radius r_p. A simple "lattice model" estimate gives us $c_p = 1/r_o^2$. The solution to the two-dimensional diffusion equation then gives

$$\tau_d = \frac{1}{2\pi D_p} \ln\left[\frac{r_0}{r_p}\right] * r_0^2 \qquad (3)$$

We note that expansion forces are neglected by Fickian diffusion. These would tend to reduce τ_d. Setting $\tau_d = \tau_{tr}$ defines a critical average distance between adsorbed peptides, r_o*, given by,

$$r_0^* = \left[\frac{2\pi}{\ln\left(r_0^*\right) - \ln\left(r_p\right)}\right]^{1/2} * H \qquad (4)$$

Assuming a typical pore radius, $r_p \sim 1$ nm gives $r_o^* \sim 7$ nm for a bilayer thickness of 4 nm. The area per lipid of DPPC bilayer is around 0.64 nm^2, this coincidentally gives a critical peptide concentration P/L* ratio of 1/150, very close to the magnitude of Huang *et al*,[61] though clearly it is derived from a completely different mechanism. The actual critical concentration will be smaller than this value, due to the thermodynamic factors, which have been ignored. For average peptide distances below this critical value, steady state diffusion of peptide through pores will be sustained at the rate $1/\tau_{tr}$. This is because, as peptides translocate through the pore, more peptides will diffuse to the pore mouth at such a rate, as to keep the pore open. At adsorption concentrations higher than the critical value, the rate-determining step is the pore crossing.

This process will begin via a nucleation event in order to create initial pores in the membrane. The probability of pore formation will depend upon lipid composition. For example, giant unilamellar vesicles (GUVs) experiments performed by Ciobanasu *et al* showed that fluorescently labeled Tat peptides could not permeate GUVs composed of zwitterionic phosphatidylcholine (PC) lipids and cholesterol only; instead, addition of 40% anionic phosphatidylserine (PS) lipids into the GUVs were found to facilitate membrane translocation of Tat peptides.[12] This suggests that the free energy of pore formation is too high for nucleation in PC lipids, which is consistent with the large values observed in our simulations (see Fig 2). On the other hand, the ability for ARG8 peptides to significantly increase pore life-times is still apparent. A similar study such as this will need to be carried out with other lipid combinations in our future work.

5. Conclusion

Molecular simulations were performed to determine if arginine-rich peptides could act cooperatively to generate and stabilize membrane pores. Our free energy calculations for pore formation by either lipid flip-flop or peptide translocation showed that the adsorption of arginine-rich peptides had little if any affect on the thermodynamic stabilization of these pores.

Hysteresis effects suggest that some stabilization is present, but more extensive simulations are likely required to obtain accurate estimates. On the other hand, it was easier to show that adsorbed peptide had a significant effect on pore life-times. A peptide had only to be present at the pore mouth to prolong the life-time sufficiently to allow it to enter the pore, over a time of 200 ns. We also found that high concentrations of ARG8 peptides can expand the membrane surface area and cause membrane thinning. We conjecture that this can cause peptide to move toward transient membrane defects such as pores in order to relieve the expansion forces. Their presence at the pores will act to prolong their life-time and this may be an important factor influencing their rapid uptake. This is certainly, the case when the surface concentration of adsorbed peptide is beyond a critical value, which allows peptide diffusion to pores over a time comparable to peptide diffusion through them. In this steady-state regime, pores will remain open. Of course, membrane compositions will significantly affect the pore-inducing behavior of arginine-rich peptides and in our future work we will study the interaction modes of arginine-rich peptides with bilayers containing anionic lipids.

Acknowledgements

An allocation time from the Lunarc Computing Center at Lund University are gratefully acknowledged. JF acknowledges funding from the Swedish Research Council

References

1. C. M. Wiethoff and C. R. Middaugh, *J. Pharm. Sci.*, 2003, **92**, 203-217.
2. M. Zorko and U. Langel, *Adv. Drug Del. Rev.*, 2005, **57**, 529-545.
3. A. D. Frankel and C. O. Pabo, *Cell*, 1988, **55**, 1189-1193.
4. E. Vives, P. Brodin and B. Lebleu, *J. Biol. Chem.*, 1997, **272**, 16010-16017.
5. S. Futaki, T. Suzuki, W. Ohashi, T. Yagami, S. Tanaka, K. Ueda and Y. Sugiura, *J. Biol. Chem.*, 2001, **276**, 5836-5840.
6. J. B. Rothbard, T. C. Jessop and P. A. Wender, *Adv. Drug Del. Rev.*, 2005, **57**, 495-504.
7. H. D. Herce and A. E. Garcia, *Proc. Natl. Acad. Sci. U. S. A.*, 2007, **104**, 10805-20810.
8. J. P. Richard, K. Melikov, E. Vives, C. Ramos, B. Verbeure, M. J. Gait, L. V. Chernomordik and B. Lebleu, *J. Biol. Chem.*, 2003, **278**, 585-590.
9. F. Duchardt, M. Fotin-Mleczek, H. Schwarz, R. Fischer and R. Brock, *Traffic*, 2007, **8**, 848-866.
10. I. Nakase, A. Tadokoro, N. Kawabata, T. Takeuchi, H. Katoh, K. Hiramoto, M. Neqishi, M. Nomizu, Y. Suqiura and S. Futaki, *Biochemistry*, 2007, **46**, 492-501.
11. J. S. Wadia, R. V. Stan and S. F. Dowdy, *Nat. Med.*, 2004, **10**, 310-315.

12. C. Ciobanasu, J. P. Siebrasse and U. Kubitscheck, *Biophys. J.*, 2010, **99**, 153-162.
13. A. Mishra, G. H. Lai, N. W. Schmidt, V. Z. Sun, A. R. Rodriguez, R. Tong, L. Tang, J. Cheng, T. J. Deming, D. T. Kamei and G. C. L. Wong, *Proc. Natl. Acad. Sci. U. S. A.*, 2011, **108**, 16883-16888.
14. N. Schmidt, A. Mishra, G. H. Lai and G. C. Wong, *FEBS Lett.*, 2010, **584**, 1806-1813.
15. M. Tang, A. J. Waring, R. I. Lehrer and M. Hong, *Angew. Chem. Int. Ed.*, 2008, **47**, 3202-3205.
16. J. B. Rothbard, T. C. Jessop, R. S. Lewis, B. A. Murray and P. A. Wender, *J. Am. Chem. Soc.*, 2004, **126**, 9506-9507.
17. H. D. Herce, A. E. Garcia, J. Litt, R. S. Kane, P. Martin, N. Enrique, A. Rebolledo and V. Milesi, *Biophys. J.*, 2009, **97**, 1917-1925.
18. S. Yesylevskyy, S. J. Marrink and A. E. Mark, *Biophys. J.*, 2009, **97**, 40-49.
19. C. Ciobanasu, E. Harms, G. Tunnemann, M. C. Cardoso and U. Kubitscheck, *Biochemistry*, 2009, **48**, 4728-4737.
20. K. Huang and A. E. García, *Biophys. J.*, 2013, **104**, 412-420.
21. W. F. D. Bennett, N. Sapay and D. P. Tieleman, *Biophys. J.*, 2014, **106**, 210-219.
22. P. A. Wender, D. J. Mitchell, K. Pattabiraman, E. T. Pelkey, L. Steinman and J. B. Rothbard, *Proc. Natl. Acad. Sci. U. S. A.*, 2000, **21**, 13003-13008.
23. B. Isralewitz, J. Baudry, J. Gullingsrud, D. Kosztin and K. Schulten, *J. Mol. Graph. Model.*, 2001, **19**, 13.
24. J. Kästner and W. Thiel, *J. Chem. Phys.*, 2005, **123**, 144104.
25. J. S. Hub, B. L. de Groot and D. van der Spoel, *J. Chem. Theory Comput.*, 2010, **6**, 3713-3720.
26. C. M. Dunkin, A. Pokorny, P. F. Almeida and H. S. Lee, *J. Phys. Chem. B*, 2011, **115**, 1188-1198.
27. M. Pourmousa and M. Karttunen, *Chem. Phys. Lipids*, 2013, **169**, 85-94.
28. O. Berger, O. Edholm and F. Jähnig, *Biophys. J.*, 1997, **72**, 2002-2013.
29. M. Vazdar, E. Wernersson, M. Khabiri, L. Cwiklik, P. Jurkiewicz, M. Hof, E. Mann, S. Kolusheva, R. Jelinek and P. Jungwirth, *J. Phys. Chem. B*, 2013, **117**, 11530-11540.
30. J. L. MacCallum, W. F. D. Bennett and D. P. Tieleman, *Biophys. J.*, 2008, **94**, 3393.
31. C. Oostenbrink, A. Villa, A. E. Mark and W. F. van Gunsteren, *J. Comput. Chem.*, 2004, **25**, 1656-1676.
32. H. J. C. Berendsen, J. P. M. Postma, W. F. van Gunsteren and J. Hermans, ed. B. Pullman, 1981.
33. J. Repáková, J. M. Holopainen, M. R. Morrow, M. C. McDonald, P. Čapková and I. Vattulainen, *Biophys. J.*, 2005, **88**.
34. W. G. Hoover, *Phys. Rev. A*, 1985, **31**, 1695-1697.
35. S. A. Nosé, *Mol. Phys.*, 1984, **52**, 255-268.
36. M. Parrinello and A. Rahman, *J. Appl. Phys.*, 1981, **52**, 7182-7190.

37. U. Essmann, L. Perera, M. L. Berkowitz, T. Darden, H. Lee and L. G. Pedersen, *J. Chem. Phys.*, 1995, **103**, 8577-8592.
38. B. Hess, H. Bekker, H. J. C. Berendsen and J. G. E. M. Fraaije, *J. Comput. Chem.*, 1997, **18**, 1463-1472.
39. S. Miyamoto and P. A. Kollman, *J. Comput. Chem.*, 1992, **13**, 952-962.
40. D. van der Spoel, E. Lindahl, B. Hess, G. Groenhof, A. E. Mark and H. J. C. Berendsen, *J. Comput. Chem.*, 2005, **26**, 1701-1718.
41. M. Z. Islam, H. Ariyama, J. M. Alam and M. Yamazaki, *Biochemistry*, 2014, **53**, 386-396.
42. S. T. Yang, E. Zaitseva, L. V. Chernomordik and K. Melikov, *Biophys. J.*, 2010, **99**, 2525-2533.
43. D. P. Tieleman, H. Leontiadou, A. E. Mark and S. J. Marrink, *J. Am. Chem. Soc.*, 2003, **125**, 6382-6383.
44. A. A. Gurtovenko and I. Vattulainen, *J. Am. Chem. Soc.*, 2005, **127**, 17570-17571.
45. Z. L. Li, H. M. Ding and Y. Q. Ma, *Soft Matter*, 2013, **9**, 1281-1286.
46. X. Chen, F. Sa'adedin, B. Deme, P. Rao and J. Bradshaw, *Biochim. Biophys. Acta*, 2013, **1828**, 1982-1988.
47. L. H. Yang, V. D. Gordon, D. R. Trinkle, N. W. Schmidt, M. A. Davis, C. DeVries, A. Som, J. E. Cronan, G. N. Tew and G. C. L. Wong, *Proc. Natl. Acad. Sci. U. S. A.*, 2008, **105**, 20595.
48. N. W. Schmidt, M. Lis, K. Zhao, G. H. Lai, A. N. Alexandrova, G. N. Tew and G. C. Wong, *J. Am. Chem. Soc.*, 2012, **134**, 19207-19216.
49. Y. C. Su, A. J. Waring, P. Ruchala and M. Hong, *Biochemistry*, 2010, **49**, 6009-6020.
50. N. B. Last and A. D. Miranker, *Proc. Natl. Acad. Sci. U. S. A.*, 2013, **110**, 6382-6387.
51. M. T. Lee, W. C. Hung, F. Y. Chen and H. W. Huang, *Proc. Natl. Acad. Sci. U. S. A.*, 2008, **105**, 5087-5092.
52. K. J. Hallock, D. K. Lee and A. Ramamoorthy, *Biophys. J.*, 2003, **84**, 3052-3060.
53. K. Matsuzaki, K. Sugishita, N. Ishibe, M. Ueha, S. Nakata, K. Miyajima and R. M. Epand, *Biochemistry*, 1998, **37**, 11856-11863.
54. P. E. Smith, J. R. Brender and A. Ramamoorthy, *J. Am. Chem. Soc.*, 2009, **131**, 4470-4478.
55. E. F. Haney, S. Nathoo, H. J. Vogel and E. J. Prenner, *Chem. Phys. Lipids*, 2010, **163**, 82-93.
56. J. L. MacCallum, W. F. D. Bennett and D. P. Tieleman, *Biophys. J.*, 2011, **101**, 110-117.
57. D. V. Zhelev and D. Needham, *Biochim. Biophys. Acta*, 1993, **1147**, 89-104.
58. H. J. Woo and A. Wallqvist, *J. Phys. Chem. B*, 2011, **115**, 8122-8129.
59. Y. Yu, J. A. Vroman, S. C. Bae and S. Granick, *J. Am. Chem. Soc.*, 2010, **132**, 195-201.
60. H. W. Huang, *Biochemistry*, 2000, **39**, 8347-8352.
61. H. W. Huang, F. Y. Chen and M. T. Lee, *Phys. Rev. Lett.*, 2004, **92**, 198304

62. P. D. Rakowska, H. B. Jiang, S. Ray, A. Pyne, B. Lamarre, M. Carr, P. J. Judge, J. Ravi, U. I. M. Gerling, B. Koksch, G. J. Martyna, B. W. Hoogenboom, A. Watts, J. Crain, C. R. M. Grovenor and M. G. Ryandov, *Proc. Natl. Acad. Sci. U. S. A.*, 2013, **110**, 8918-8923.